Corrosion Performance of Alumina Scales in Coal Gasification Environments*

K. Natesan
Energy Technology Division
Argonne National Laboratory
9700 S. Cass Avenue
Argonne, IL 60439

February 1997

DISCLAIMER

Invited paper for presentation at the Second International Workshop on Corrosion in Advanced Power Plants, Tampa, FL, March 3-6, 1997.

*Work supported by the U.S. Department of Energy, Office of Fossil Energy, Advanced Research and Special Technologies Materials Program, Work Breakdown Structure Element ANL–4, under Contract W–31–109–Eng–38.

Corrosion Performance of Alumina Scales in Coal Gasification Environments

K. Natesan
Argonne National Laboratory
9700 S. Cass Avenue
Argonne, IL 60439

Abstract

Corrosion of metallic structural materials in complex gas environments of coal gasification is a potential problem. The corrosion process is dictated by concentrations of two key constituents: sulfur as H_2S and Cl as HCl. This paper examines the corrosion performance of alumina scales that are thermally grown on Fe-base alloys during exposure to O/S mixed-gas environments. The results are compared with the performance of chromia-forming alloys in similar environments. The paper also discusses the available information on corrosion performance of alloys whose surfaces were enriched with Al by the pack-diffusion process, by the electrospark deposition process, or by weld overlay techniques.

Introduction

Coal gasification technologies emphasize production of intermediate-Btu syngas by using oxygen and steam to gasify coal. The syngas is used as a feedstock for chemical production or is burned to provide industrial process heat, steam and/or electricity. Three different types of gasifiers — fixed-bed, fluidized-bed and entrained slagging-bed — are being considered. In dry-ash gasifiers, metallic alloys with lifetimes of at least 20,000 h are required for use in gasifier internal components. In the case of slagging gasifiers, no metallic internals will be used because gasification occurs at a much higher temperature, but metallic cyclones and heat-recovery systems (also called syngas coolers) are needed outside the gasifier vessel.

In the last workshop, it was concluded that reliable materials performance is of critical importance in moving integrated gasification combined cycle (IGCC) power generation from the demonstration phase to full commercial utilization.[1] A discussion was held on the extent to which selection or development of new materials would reduce the cost of coal gasifiers. Although it was agreed that gold plating and excessive redundancy should be avoided, it was generally concluded that the scope for large cost reductions through the use of cheaper materials is limited. The workshop also concluded that the primary goal in the materials area is to identify a material that is resistant to corrosive attack by a wide range of coal gasification atmospheres containing H_2S, COS, HCl, slag, and ash particles, etc., at temperatures

of 200-600°C. However, it was stipulated that the material cost should be similar to that of low-alloy steel. The delegates affiliated with plant operation emphasized the need for low-cost materials to improve plant economics, but panel discussions on the subject questioned this requirement. The panel concluded that the gasifier and syngas cooler represent <25% of the total plant cost, and that it was difficult to see how a reduction in the cost of high-temperature metallics (especially for syngas cooler application) could make a significant improvement in plant economics, particularly if materials costs are considered from a life-cycle basis.

A key materials issue in coal gasification is the corrosion performance of structural alloys used for the syngas cooler. The biggest corrosion problem is sulfidation of the alloys in multicomponent gaseous environments and its interplay with oxidation and chloridation. In addition to the gaseous corrosion, the performance of materials subjected to downtime conditions and coal slag environments is also of concern. Corrosion performance of two classes of alloys, namely, carbon and low-alloy steels, which form sulfide scales, and high-chromium austenitic alloys, which form chromia/Cr sulfide scales, was discussed in the last workshop. It is well known that carbon and low-alloy steels do not form protective oxide scales and sulfidize only in the low-pO_2 and moderate-to-high pS_2 environments of coal gasification processes. The scale generally consists of FeS, and the sulfidation rate is fairly rapid because of the high diffusivity of Fe in the sulfide phase. The sulfidation rate is dictated by the partial pressure of H_2S in the exposure environment, which ranges from 0.5-1.0 vol.% based on the sulfur content of the U.S. coal feedstocks, and exposure temperature. Therefore, the application of these alloys is determined by the corrosion losses tolerable for the designed service life of the components, H_2S content of the gas, and temperature.

The second class of alloys that has been heavily corrosion-tested is austenitic Fe-Cr-Ni alloys, which generally form Cr oxides and/or Cr sulfides depending on the pO_2 and pS_2 in the exposure environment. Some of the alloys in this class include Alloy 800, Types 304, 316 and 310 stainless steel, and others. In highly oxidizing atmospheres, these alloys develop chromia scales and their corrosion resistance is fairly good, even in the presence of H_2S. It has been established in the literature that the threshold pO_2 to form stable chromia scale in these alloys is at least 2 to 3 orders of magnitude higher than the equilibrium pO_2 for the chromia/Cr sulfide phase boundary at >750°C and may be 4-5 orders of magnitude higher at 400-650°C.[2] The failure of the chromia scales in O/S mixed gas environments has been attributed to the presence of microchannels and cracks through which S transports inward through the scale, while cations such as Fe migrate outward and form FeS phase, eventually destroying the originally developed protective chromia scale. Generally, development of chromia scale substantially reduces corrosion rates relative to those for low-alloy

steels that form FeS scale. However, in environments that contain pO_2 < threshold pO_2, even the high-Cr alloys develop only sulfide scales, predominantly Cr sulfide or (Fe,Cr) sulfide. Under these conditions, scaling rates are high and again the application of the alloys is dictated by the metal wastage acceptable in service that, in turn, is dictated by temperature and H_2S content of the exposure environment.

The purpose of this paper is to evaluate the corrosion performance of alumina-forming alloys for service in coal-gasification environments and examine application procedures to increase Al concentrations in the surface regions of engineering alloys, thereby improving their corrosion resistance.

Coal Gasification Environment

In coal-gasification systems, the gas environment is characterized by low pO_2 and moderate-to-high pS_2 and the S is present as H_2S. The environment is represented by thermochemical diagrams, as depicted in Fig. 1 by the hatched boxes for 400 and 650°C.[3] The effect of the gas chemistries on the corrosion of structural materials and the stability of various corrosion-product phases can be determined from the O/S partial pressures with the thermochemical diagrams shown in Fig. 1. At 400°C, the Fe-, Ni-, and Co-base alloys are expected to form sulfide scales and Cl in the environment can exacerbate the corrosion of these materials. At 650°C, alloys can develop chromia scale in high Cr alloys but in carbon/low-alloy steels, FeS will be the predominant phase in the scale. On the other hand, alloys with high Al content have the potential to develop alumina scale and offer corrosion protection, if they are mechanically bonded to the substrate. The pO_2 and pS_2 values in the gasification environments are such that these values are at least 6 to 10 orders of magnitude higher than that established by Al_2O_3/Al_2S_3 equilibrium. The scaling process will be dictated by the relative growth kinetics of alumina and transient oxides such as Fe and Cr oxides.

Characteristics of Alumina Scales

The only thermodynamically stable solid oxide in the Al-O system is Al_2O_3 (melting point 2072°C). Various structural forms of the oxide are possible and the stability of different oxide forms is dictated by temperature. While Cr_2O_3 normally exhibits p-type electrical behavior in which Cr is mobile, alumina exhibits more complex electrical properties whereby either Al or O may be mobile. Based on the bulk self-diffusion data in polycrystalline material depicted in Fig. 2, the rate of Cr_2O_3 scale formation would be expected to exceed the rate of Al_2O_3 scale formation by more than six orders of magnitude at temperatures <1200°C, assuming growth to be contolled by cation diffusion in each case. Extrapolation of the diffusion data to lower temperatures

indicates that below ≈1275°C, the rate of anion diffusion will exceed the rate of cation diffusion. Below ≈900°C, the alumina is generally formed as γ–Al_2O_3 and the corrosion protection of this alumina is not well established.[4]

A comparative analysis of growth rates of Cr_2O_3 and Al_2O_3 scales was made by Hindam and Whittle.[5] The scaling-rate constants shown in Fig. 3 as a function of temperature indicate significant scatter in the data for chromia scale formed in different alloys and less scatter for formation of alumina. However, the results clearly show that the scaling rates for alumina are at least a few orders of magnitude lower than for chromia, especially at lower temperatures. One concern is that the alumina scaling rate is so low that transient oxides of Fe, Ni, and Cr may be present in the corrosion product scale for a long period of exposure and thus the benefit of slow-growing alumina for corrosion protection may not be realized in practice.

Oxygen partial pressure appears to have little influence on the rate of Al_2O_3 scale formation,[6] but impurities may dope the oxide and influence its growth characteristics,[7] permit formation of spinel oxides, and play a vital role in the mechanical behavior of Al-rich oxide scale. The rate of S diffusion through Al_2O_3 can be 1 to 4 orders of magnitude greater than the rate of O diffusion, depending on oxide grain size (see Fig. 4), but may be 1.5 to 4.5 orders of magnitude lower than the rate of S diffusion through Cr_2O_3.[8] In both oxides, however, the partial pressures of S_2 and O_2 will determine whether sulfidation is induced and scale breakdown occurs.[9]

Oxidation Behavior of Al-Containing Alloys

In Ni-Al, Fe-Al, and Co-Al binary alloys, an Al content in excess of 10 wt.% is normally needed to support formation of a surface Al_2O_3 scale.[10] The presence of Cr reduces the amount of Al required to form Al_2O_3 (to 3-5 wt.%).[11] Chromium minimizes internal oxidation of Al by acting as an oxygen getter,[12] but when it is present in high concentrations (>25 wt.% in Fe-Cr-Al alloys), ductility and workability of the alloy are impaired.[13] The commercially available structural alloys that form alumina scale generally also contain a fairly high concentration of Cr. In these alloys, the Cr-Al ratio appears to dictate the scaling kinetics and long-term mechanical integrity of the scale. A combination of good mechanical properties and oxidation resistance is generally obtained by optimizing the alloy chemistry. A Cr content of 20 wt.% or more is necessary to support alumina scale formation with only 5 wt.% Al. In the case of structural alloys, sufficient Ni in the alloy ensures austenite stability (providing creep strength) while maximizing the Fe content reduces cost. Alloy grain size is important in quarternary Fe-Cr-Ni-Al alloys in promoting alumina formation unless a second phase is present.[14]

Mechanical stability or the lack of it is a well-known problem associated with alumina scales. Scales composed of alumina commonly exhibit mechanical instability, e.g., cracking, spallation, and delamination, which poses a serious drawback in the application of Al_2O_3-forming alloys. The growth of a surface scale under isothermal or thermal-cycling conditions inevitably results in the generation of stress.[15] Compressive stresses will accumulate in a scale until some critical point is reached at which relief of stress must occur. If adhesion is poor, as it may be in many thermally grown Al_2O_3 scales, localized scale buckling may result in tensile fracture. The loss of corrosion resistance depends on the level of applied stress and also on the initial level of stress in the scale and the amount of deformation that can be accommodated. The area of metal surface exposed by scale cracking and the ability of the alloy to reform a protective scale will influence the rate of alloy degradation.

To examine the adhesion of thermally grown alumina scales to the substrate, Natesan et al.[16] applied a tensile pull to separate the scale from the substrate. The technique they used involves attaching an epoxy-coated pin to the scale surface at a temperature sufficient to cure the epoxy. The pin is subsequently separated from the sample at room temperature by applying a tensile load. The surfaces of the pulled pins are then examined to assess whether the debonding occurred in the scale itself or at the scale/metal interface. The strength of the epoxy, and hence the maximum strength measurable by this procedure, was ≈71 MPa. If the applied load and pin area of contact are known, the stresses needed to pull the scale from the substrate can be calculated. The results indicate a substantial scatter in the data from oxidized specimens. It is believed that for many samples (especially for those prone to oxide spallation), voids or variations in the topography of the oxide layer result in an incomplete bond between the oxide and the epoxy-coated pin. Furthermore, in some of the samples, the separation between the pin and the oxide occurred in the oxide itself rather than at the oxide/alloy interface.

Figure 5 shows the maximum stress endured by the scales on several alumina-forming alloys oxidized at 800, 1000, and 1200°C. Alloy FA 186 is a ternary alloy that contained Fe, Cr, and Al and is considered a base alloy. Alloy FA 129 is designed to exhibit high ductility at room temperature while retaining its strength at high temperatures, whereas FAL is designed for improved oxidation resistance through addition of Zr. Alloy FAS is designed to resist sulfidation, and FAX is designed for improved resistance in aqueous environments by deliberate addition of Mo. The results show a peak in maximum stress value for specimens of FAS, FA 186, and FA 129 exposed at 1000°C. On the other hand, maximum stress values for FAL and FAX specimens are almost independent of exposure temperature. The adhesion test results from FAL and FAX also indicate that even with a wide variation in the oxide layer thickness (resulting from oxidation for 100 h at 800-1200°C), the tensile stress

needed to pull the sample from the substrate is fairly independent of oxide thickness. The difference in the stress values for FAL and FAX must be due to differences in the chemistry in the scale and in the scale/alloy interface, which are directly influenced by the initial composition of the substrate alloy. The results also show that Zr (in FAL) and Nb (in FA 129) additions have a similar effect at 1000 and 1200°C, where α-Al_2O_3 will be the stable oxide in the scale. A comparison of the results obtained from these two alloys after 800°C oxidation indicates that addition of Zr, rather than Nb, may stabilize the alumina scale (i.e., minimize the transient oxides) on the alloy surface. Similar information is presently not available on alumina developed at the low temperatures of interest in coal-gasification systems.

Behavior of Alumina Scales in Coal Gasification Environments

Extensive studies have been conducted on the corrosion performance of alumina-forming alloys in O/S mixed-gas environments.[17-20] Nickel-base alloys are susceptible to sulfidation attack and rarely perform well in S-containing environments. Therefore, corrosion studies have focused on Fe-base alumina-forming alloys. Figure 6 shows weight change data from thermogravimetric analysis (TGA) of several Fe-Al binary alloys and Fe_3Al tested in an O/S mixed-gas environment at 875°C. The results indicate significant corrosion of alloys with 8 and 10 wt.% Al, whereas the alloy with 12 wt.% Al and Fe_3Al (with 13.9 wt.% Al) exhibited negligible corrosion under the same conditions. Figure 7 shows scanning electron microscopy (SEM) photomicrographs of cross sections of Fe-Al binary alloys and Fe_3Al after exposure to a mixed-gas environment. Energy-dispersive X-ray analysis showed that the alloys with 8 and 10 wt.% Al developed predominantly Fe sulfide scale, whereas the other two alloys developed Al oxide scale. The 8 wt.% Al alloy was tested for only 1.75 h, whereas the 10 wt.% Al alloy was tested for 5.5 h; as a result, the absolute values of the scale thicknesses should not be compared. However, both alloys appear to undergo catastrophic sulfidation in the O/S mixed gas with S levels that are anticipated in gasification systems that use high-S coal as feedstock. Figure 7 also shows that the 12 wt.% Al and Fe_3Al alloys develop extremely thin scales after ≈90 h of exposure to the mixed-gas environment.

Figure 8 shows TGA weight-change data for several high-purity Fe-Cr, Fe-Cr-Ni, Fe-Al, and Fe-Cr-Al alloys and Fe_3Al after exposure to an O/S mixed-gas environment at 875°C. Data for the Fe-Cr binary alloy show that Cr concentration at the high level of 25 wt.% does not improve the sulfidation resistance of the alloy, which develops a scale (consisting of a mixture of Fe and Cr sulfide) at a very high growth rate. Addition of 20 wt.% Ni to this alloy does not improve its corrosion resistance. In fact, the presence of Ni leads to the formation of the Ni-Ni_3S_2 eutectic if the test is run for a longer time. The composition of this ternary alloy is similar to the base composition of

Type 310 stainless steel and its behavior is similar, as reported earlier.[17] The weight change behavior of Fe-10 wt.% Al alloy is similar to that of Fe-Cr and Fe-Cr-Ni alloys. An addition of 6 wt.% Al to the Fe-25Cr alloy seems to reduce the corrosion rate somewhat but the external scale consists of Fe sulfide, which is not expected to offer protection against breakaway corrosion. The binary Fe-12 wt.% Al alloy and Fe_3Al (with 13.9 wt.% Al) exhibit superior corrosion resistance in O/S mixed-gas atmospheres. The scales on these alloys were Al oxide and contained little S. The results indicate that a critical Al content in excess of 10 wt.%, which is present in Fe aluminides, is needed for alumina formation on the alloy surface in environments typical of coal-gasification systems.

Weight change data for several Al-containing commercial alloys, along with data for Fe-12 wt.% Al and Fe_3Al alloys, are shown in Fig. 9. The alloy 8XX, which contains ≈3-4 wt.% Al, exhibited catastrophic corrosion, as expected. The alloys GE 1541 and RV 8413 are Fe-based alloys with moderate Cr content and ≈5-6 wt.% Al. Corrosion performance of these alloys is not adequate for service in coal-gasifier environments.

Surface Enrichment with Al for Corrosion Resistance

Even though the corrosion resistance of Fe-base alloys with high Al content is significant in environments that are prevalent in fossil energy systems, the use of these alloys as structural materials at elevated temperatures is very limited because of their inadequate strength properties and fabrication difficulties. Several approaches have been examined to enrich the surface regions of conventional structural alloys with Al which can form alumina scale during service, thereby offering improved corrosion protection. Two of the approaches for Al enrichment are the pack diffusion and weld overlay processes.

In pack diffusion, alloy samples are enclosed in a pack that consists of appropriate alloy powders, inert refractory powders, and a halide activator; the pack is heated to elevated temperature for time sufficient to transport the desired coating element, Al, from the pack to the alloy surface. Aluminizing, chromizing, and simultaneous chromizing and aluminizing coatings are often prepared by this approach.

In the weld overlay process, claddings of high Al contents are produced by electrospark-deposition (ESD) and by gas tungsten arc and gas metal arc techniques. The ESD process is a microwelding technique that uses short-duration, high-current electrical pulses to deposit an electrode material on a metallic substrate. A principal advantage of the ESD process is that the overlay is fused to the metal surface with low heat input while the bulk substrate material remains at ambient temperature. This eliminates thermal distortion or changes in the metallurgical structure of the substrate. Because the overlay is alloyed with the surface, i.e.,

metallurgically bonded, it is inherently more resistant to damage and spalling than the mechanically bonded coatings produced by most other low–heat–input processes (such as detonation–gun, plasma–spray, and electrochemical plating). The use of welding to produce Fe aluminide layers leads to a loss of selected elements by vaporization and significant mixing of the filler metal and substrate alloys (dilution) during deposition. Because the substrates contain essentially no Al, the concentration of this element in the overlay is generally much lower than it is in the welding rod/wire used to produce the overlay.

Corrosion Performance of Pack Diffusion Coatings

Substantial work has been conducted to evaluate the corrosion behavior of aluminized, chromized, simultaneously aluminized and chromized, and sequentially aluminized/chromized coatings exposed to simulated O/S mixed gas environments.[21-23] Coatings were applied on low-alloy (1.25 and 2.25 wt.% Cr) and 9 wt.% Cr ferritic steels and austenitic alloys, such as Type 304 stainless steel and Alloy 800. A test program was conducted to evaluate the sulfidation resistance of the coated specimens and to compare their corrosion resistance with that of uncoated ferritic steels and austenitic alloys.[23] These tests were conducted for 500-2000 h with internally air-cooled specimens at metal temperatures of 500 and 650°C and the gas was maintained at 871°C. The oxygen/sulfur mixed-gas environments in these tests had pO_2 values of 9.2×10^{-28} and 1.2×10^{-23} atm and pS_2 values of 7.7×10^{-8} and 1.0×10^{-6} atm, respectively, at 500 and 650°C.

Figure 10 shows corrosion loss data for several uncoated and coated specimens from this test program. The scales on the ferritic steels consisted predominantly of iron sulfide and (Fe,Cr) sulfide while the high-Cr alloys developed somewhat thinner (Cr,Fe) sulfide scales with intergranular penetration of sulfur into the alloy. The results showed that alloy T22 had corrosion losses of 3.3 and 11.8 mm/yr (based on linear kinetics) at 500 and 650°C, respectively. The corresponding values for T91 alloy were 1 and 3.5 mm/yr at 500 and 650°C. On the other hand, corrosion losses for high-Cr alloys ranged from 0.2 to 1.0 mm/yr (also based on linear kinetics). The chromized, aluminized, and simultaneously chromized-aluminized samples exhibited substantial decrease in sulfidation attack and metal wastage via corrosion relative to those of the uncoated T22 alloy. The specimen with a chromized coating developed a thin chromium sulfide scale with a thickness only about 20% of that of the chromized layer. The specimen with an aluminized coating exhibited a thinner scale that contained Fe, Al, and S. The simultaneously chromized–aluminized specimen developed a thin (Fe,Cr) sulfide scale but the zone underneath the scale was enriched in Cr and Al but contained virtually no Fe. This zone seemed to act as a barrier to Fe transport

outward, thereby lowering susceptibility to formation of fast–growing FeS and minimizing corrosion loss.

Corrosion Performance of ESD Layers

Several specimens with Al-enriched surfaces, applied on Type 316 stainless steel and Alloy 800 substrate alloys by the ESD process, were tested in simulated gasification environments that contained H_2S with or without HCl. In the first experiment, performance of the ESD coatings (which included Fe_3Al with differing bond coats of refractory metals and/or noble metals) was compared with that of uncoated austenitic alloys.[24] Figure 11 shows corrosion loss data obtained for specimens tested for 1000 h at 650°C in gas mixtures where $pO_2 = 1.2 \times 10^{-23}$, $pS_2 = 5.2 \times 10^{-10}$, $pCl_2 = 9.4 \times 10^{-17}$, and $pHCl = 2.1 \times 10^{-3}$ atm. All of the Fe aluminide coatings were resistant to sulfidation and chloride attack, whereas the base alloys were susceptible to general corrosion and pitting attack, especially in the HCl-containing environment. The weight change data and extensive microscopic analyses of tested specimens showed that the bond coats themselves do not significantly influence the corrosion process.

Further evaluation of Fe aluminide coatings was conducted with a Type 316 stainless steel substrate coated with either Fe_3Al or FeAl welding rod.[25] Coatings made with FeAl welding rod contained much more Al than those made with Fe_3Al welding rod. Type 316 stainless steel specimens with and without coatings and several commercial high-Cr alloys were exposed to O/S mixed-gas environments for up to 728 h and periodically retrieved to measure weight changes at intermediate exposure times. Figure 12 shows weight change data for Alloy 800 and Type 316 stainless steel and for Fe_3Al- or FeAl-coated Type 316 stainless steel as a function of exposure time at 650°C to simulated gasification environments with or without HCl. The uncoated alloys exhibited some general corrosion and significant sulfidation and localized pitting corrosion. Weight gains and scaling rates were much lower for the aluminide-coated specimens than for the uncoated Type 316 stainless steel and Alloy 800.

Figure 13 shows similar weight change data for several commercial high-Cr alloys exposed together with FeAl-coated Type 316 stainless steel in O/S mixed-gas environments with and without HCl. The corrosion performance of the FeAl-coated specimen is comparable to or better than those of most other materials tested. Further, the cost of materials such as HR 160 and Alloy 556, which exhibit corrosion rates similar to FeAl layered specimen, will be a factor of 5 to 10 times higher than the FeAl coated specimen. Figure 14 shows corrosion loss data for several of these alloys and coatings calculated by parabolic kinetics. Limited number of corrosion experiments were also conducted with Al-enriched alloys in the presence of coal slag derived

under substoichiometric combustion conditions. The glassy slag had a composition (in wt.%) of 50 SiO_2, 21 Al_2O_3, 11 Fe_2O_3, 13 CaO, 2.5 MgO, 0.25 Na_2O, O.7 K_2O, and 1.0 TiO_2. Figure 15 shows weight change data for Fe-12Al and Fe_3Al alloys from thermogravimetric tests. In the presence of slag, the alloy seems to react early during exposure and subsequently reaches a plateau in weight change, indicating very little reaction.

Corrosion Performance of Weld Overlay Claddings

Iron aluminide overlays were also prepared by gas tungsten arc and gas metal arc techniques.[26] Several specimens of Fe aluminide overlay were exposed to oxidizing/sulfidizing gas environments at 800°C in isothermal tests. Results showed that the corrosion performance of overlays that contained >21 at.% Al was superior to that of conventional Fe-Cr-Ni and Fe-Cr-Al alloys. However, a rapid degradation in corrosion resistance was observed under thermal cycling conditions when the initially grown scales spalled and the subsequent rate of reaction was not controlled by the formation of slow-growing alumina. It was concluded that Al concentrations >25 at.% are needed to ensure adequate corrosion resistance in mixed-gas environments.

Summary

The raw gas environments that arise from gasification of coal have chemical compositions that are low in pO_2 and moderate -to- high in pS_2. Metallic materials for service in such environments undergo predominantly sulfidation attack at temperatures of 400-700°C. Further, the gasification environments contain HCl, the concentration of which is determined by the chlorine content of the coal feedstock. In addition, the metallic materials must be resistant to attack by coal-slag particles that are carried by the gas and generally deposited onto the cooler surfaces of the syngas cooler. The paper examines in detail the corrosion performance of alumina scales in complex environments that contain S and Cl. Experimental data on binary Fe-Al alloys showed that a threshold Al concentration of at least 10 wt.% is needed to minimize corrosion in these environments. Further, surface enrichment of conventional structural alloys with Al-enriched surfaces produced by pack diffusion and electrospark deposition improved corrosion resistance in simulated coal gasification environments that contained S and/or Cl, as well as in the presence of coal slag.

Acknowledgments

This work was supported by the U.S. Department of Energy, Office of Fossil Energy, Advanced Research and Special Technologies Materials Program, under Contract W-31-109-Eng-38.

References

1. Proc. 1st Int. Workshop on Materials for Coal Gasification Power Plant, Petten, The Netherlands, June 14-16, 1993, eds. J. F. Norton and W. T. Bakker, Butterworth-Heinemann, Oxford, U.K., Mater. at High Temps. 11, 1993.
2. T. C. Tiearney, Jr., and K. Natesan, Oxid. Met. 14, 363, 1980.
3. K. Natesan, ibid, p. 36.
4. G. C. Wood and F. H. Stott, in High Temperature Corrosion, ed. R. A. Rapp, NACE, Houston, TX, 1983.
5. H. Hindam and D. P. Whittle, Oxid. Met. 18, 245, 1982.
6. T. A. Ramanarayanan, M. Raghavan, and R. Petrovic-Luton, Trans. Jap. Inst. Met. 34, 199, 1983.
7. P. A. Lessing and R. S. Gordon, J. Mater. Sci. 12, 2291, 1977.
8. J. B. Wagner, Defects and Transport on Oxides, p. 283, Plenum, New York, 1973.
9. P. A. Mari, J. M. Chaix, and J. P. Larpin, Oxid. Met. 17, 315, 1982.
10. G. N. Irving, J. Stringer, and D. P. Whittle, Oxid. Met. 9, 427, 1975.
11. G. R. Wallwork and A. Z. Hed, Oxid. Met. 3, 171, 1971.
12. G. C. Wood and M. G. Hobby, Proc. 3rd Int. Cong. on Metallic Corrosion, Moscow, p. 102, 1966.
13. C. S. Wukusick and J. F. Collins, Mat. Sci. Stand., 637, 1964.
14. D. Delaunay and A. M. Huntz, J. Mater. Sci. 18, 189, 1983.
15. I. Pfeiffer, Z. Metallkunde, 53, 309, 1962.
16. K. Natesan, K. Klug, D. Renusch, B. W. Veal, and M. Grimsditch, Microstructural and Mechanical Characterization of Alumina Scales Thermally Developed on Iron Aluminide Alloys, Argonne National Laboratory Report ANL/FE-96/01, 1996.
17. K. Natesan, in Proc. 7th Annual Conf. Fossil Energy Materials, ORNL/FMP-93/1, p. 249, 1993.
18. K. Natesan and W. D. Cho, in Proc. 8th Annual Conf. Fossil Energy Materials, ORNL/FMP-94/1, p. 227, 1994.
19. K. Natesan and R. N. Johnson, in Proc. 2nd Int. Conf. Heat-Resistant Materials, eds. K. Natesan, P. Ganesan, and G. Lai, p. 591, ASM International, Materials Park, OH, 1995.
20. P. F. Tortorelli and J. H. DeVan, Mater. Sci. and Eng., A153, 573, 1992.

21. D. J. Baxter, The Corrosion Behavior of Coated Low-Alloy Steels in a Coal Gasifier Environment Under Thermal-Cycling Conditions, Argonne National Laboratory Report ANL/FE-86-6, 1986.
22. D. J. Baxter, High Temp. Technol. 4, 207. 1986.
23. K. Natesan and R. N. Johnson, Surface and Coatings Technology, 43/44, 821, 1990.
24. K. Natesan, Materials at High Temperatures, 11, 36, 1993.
25. K. Natesan and R. N. Johnson, in Proc. 2nd Intl. Conf. Heat-Resistant Materials, K. Natesan, P. Ganesan, and G. Lai, Eds., p. 591, ASM International, Materials Park, OH, 1995.
26. P. F. Tortorelli, B. A. Pint, and I. G. Wright, in Proc. 10th Annual Conf. Fossil Energy Materials, Oak Ridge, TN, ORNL/FMP-96/1, p. 393, 1996.

Table 1. Nominal Chemical Composition (in wt.%) of Alloys Cited in This Paper

Material	C	Cr	Ni	Mn	Si	Mo	Al	Fe	Other
C steel	0.18	–	–	0.5	0.25	–	–	Bal[a]	–
T11	0.10	1.23	–	0.8	0.3	0.50	–	Bal	–
T22	0.12	2.30	0.1	0.4	0.3	1.0	–	Bal	–
T91	0.08	8.57	0.09	0.46	0.4	1.0	-	Bal	-
304	0.08	18.3	8.1	1.50	0.27	0.27	-	Bal	-
316	0.05	17.4	13.8	1.5	0.73	2.2	-	Bal	-
310	0.07	25.0	18.7	1.21	0.64	0.002	-	Bal	-
800	0.08	20.1	31.7	0.96	0.24	0.30	0.39	Bal	Ti 0.31
8XX	-	20.2	32.5	-	-	–	3.0	Bal	–
GE 1541	-	15.2	-	0.001	0.07	-	4.95	Bal	Y 0.7
RV 8413	-	18.5	0.06	0.001	0.025	-	5.91	Bal	Hf 0.5
HR 160	0.05	28.0	Bal	0.5	2.75	–	–	4.0	Co 27.0
Alloy 556	0.10	22.0	20.0	1.5	0.4	3.0	-	Bal	Co 20.0, W 2.5
253 MA	0.10	20.7	10.9	0.3	1.8	-	–	Bal	Ce 0.03
FA 186	-	2.2	-	-	-	-	15.9	Bal	-
FAS	-	2.2	-	-	-	-	15.9	Bal	B 0.01
FA129	-	5.5	-	-	-	-	15.9	Bal	Nb 1.0, C 0.05
FAL	-	5.5	-	-	-	-	15.9	Bal	Zr 0.1, B 0.05
FAX	-	5.5	-	-	-	-	15.9	Bal	Nb 1.0, Mo 1.0, Zr 0.15, B 0.04
Fe_3Al	-	-	-	-	-	-	13.9	Bal	-
FeAl	-	-	-	-	-	-	34.0	Bal	-
Fe-8Al	-	-	-	-	-	-	8.0	Bal	-
Fe-10Al	-	-	-	-	-	-	10.0	Bal	-
Fe-12Al	-	-	-	-	-	-	12.0	Bal	-
Fe-25Cr	-	25.0	<0.01	<0.01	<0.01	-	<0.01	Bal	-
Fe-25Cr-20Ni	-	24.8	19.9	<0.01	<0.01	-	0.01	Bal	-
Fe-25Cr-6Al	-	24.6	<0.01	<0.01	<0.01	-	5.9	Bal	-

[a]Indicates balance.

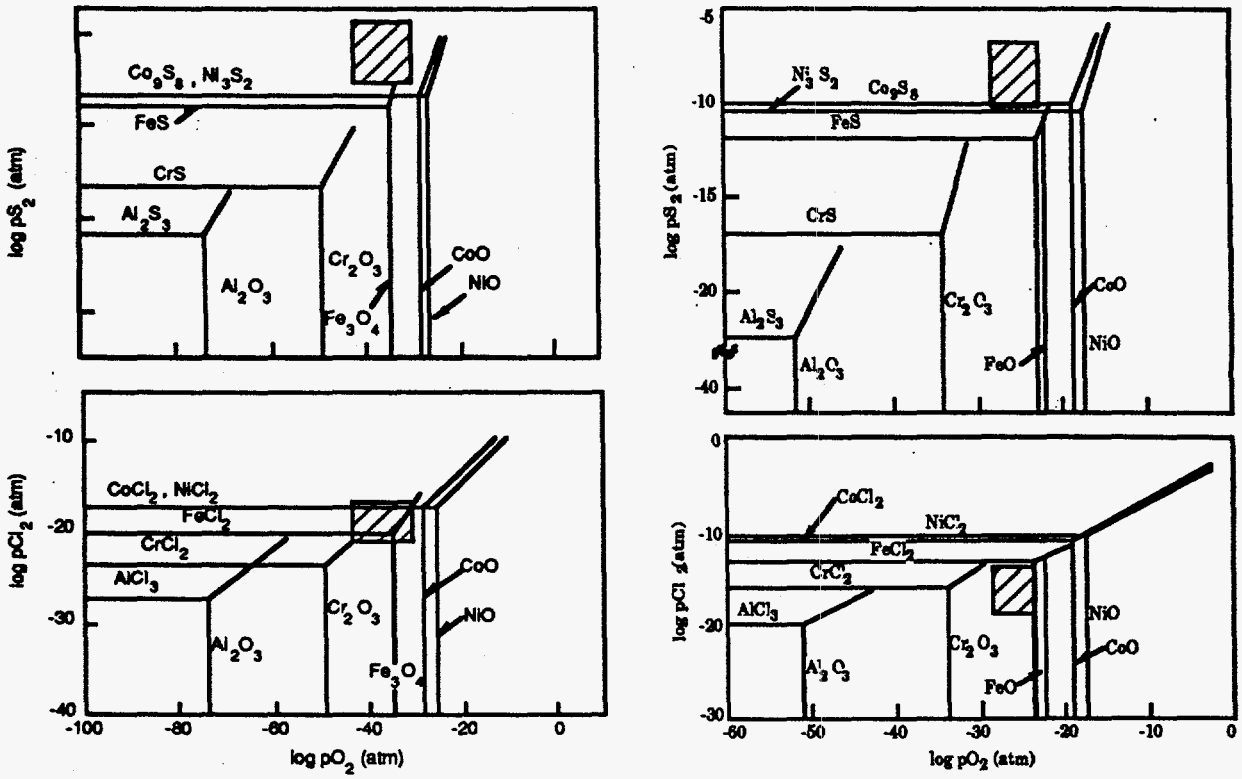

Figure 1. Oxygen/sulfur and oxygen/chlorine thermochemical diagrams for several metals, calculated for (left) 400°C and (right) 650°C. Also shown are regions (in hatched boxes) of coal gasification process environments.

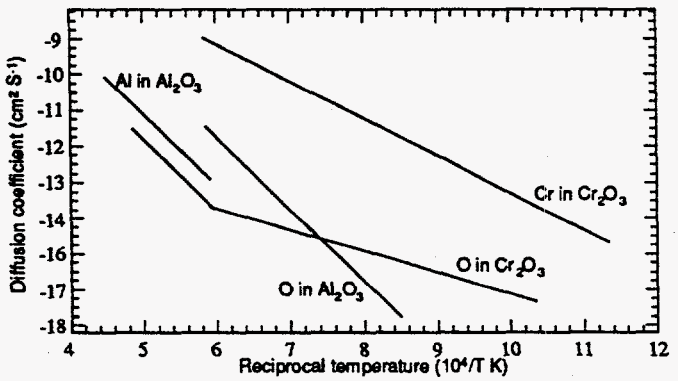

Figure 2. Self-diffusion data in chromia and alumina.

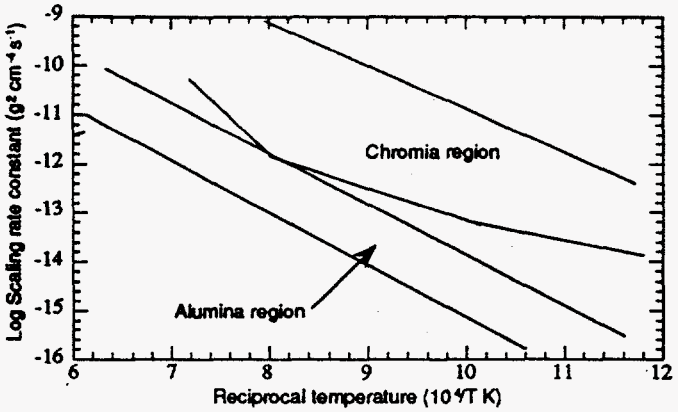

Figure 3. Scaling-rate constants for formation of alumina and chromia scales (based on data from Ref. 5)

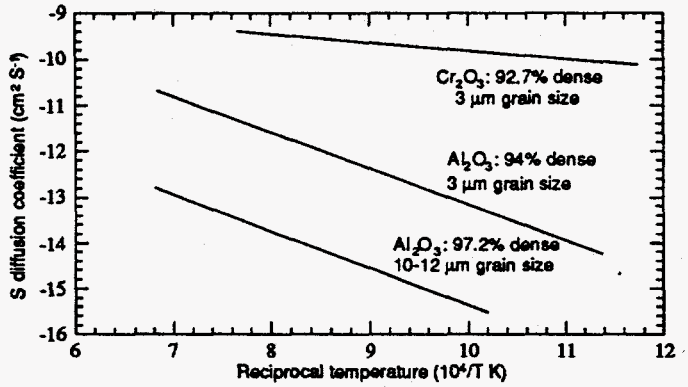

Figure 4. Rates of sulfur diffusion in alumina and chromia (based on data from Ref. 11).

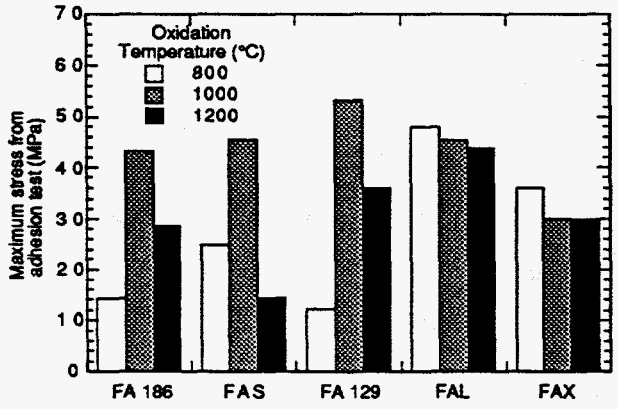

Fig. 5. Maximum stress needed to pull scale from substrate for oxides that developed on several Fe-Al alloys oxidized at 800, 1000, and 1200°C.

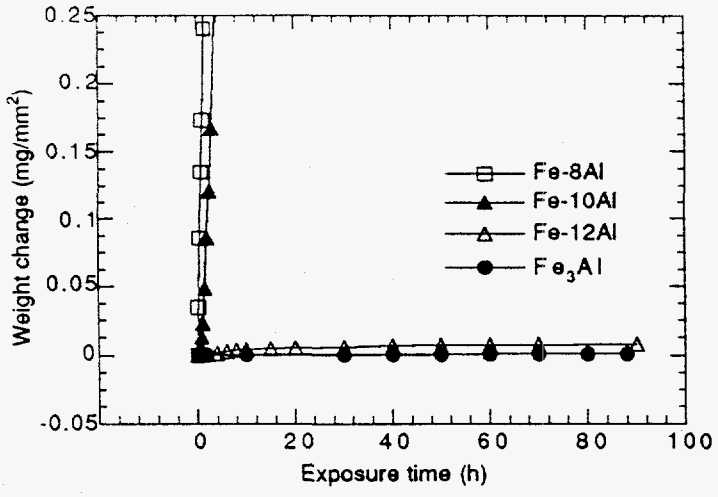

Figure 6. Weight-change data for Fe-Al binary alloys and iron aluminide specimens tested in oxygen/sulfur mixed gas at 875°C.

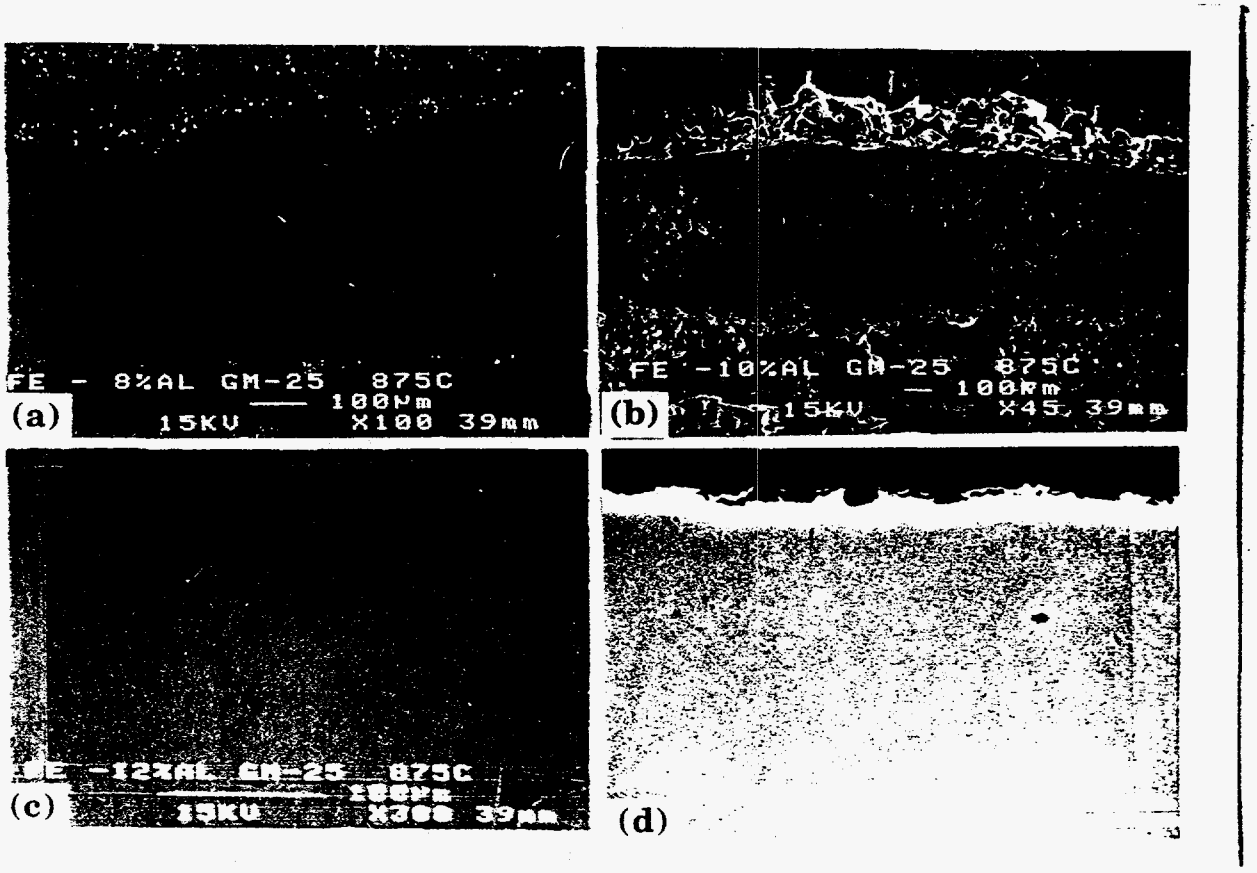

Figure 7. SEM photomicrographs of cross sections of (a) Fe-8 wt.% Al, (b) Fe-10 wt.% Al, (c) Fe-12 wt.% Al, and (d) Fe_3Al specimens after exposure in O/S environment with $pO_2 = 4.1 \times 10^{-18}$ and $pS_2 = 9.4 \times 10^{-7}$ atm at 875°C.

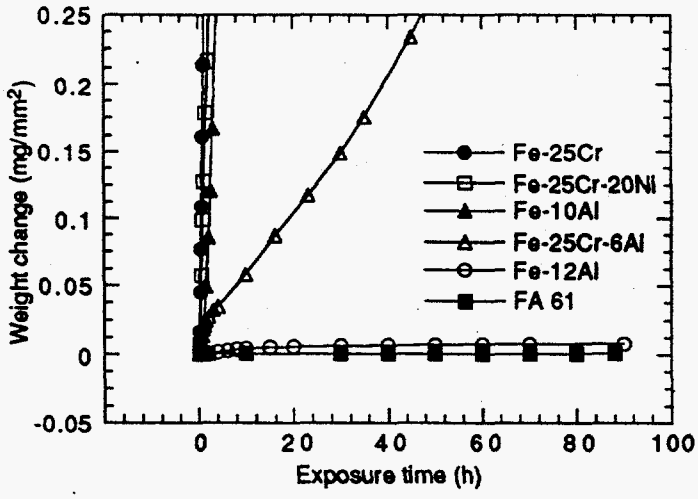

Figure 8. Weight change data for Fe-Cr, Fe-Cr-Ni, Fe-Al, and Fe-Cr-Al alloys and Fe_3Al tested in O/S environment with $pO_2 = 4.1 \times 10^{-18}$ and $pS_2 = 9.4 \times 10^{-7}$ atm at 875°C.

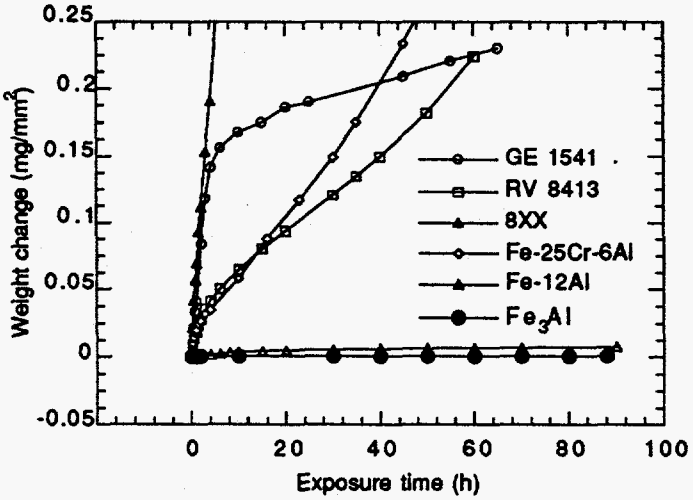

Figure 9. Weight change data for several commercial alloys, Fe-12Al alloy, and Fe_3Al tested in O/S environment with $pO_2 = 4.1 \times 10^{-18}$ and $pS_2 = 9.4 \times 10^{-7}$ atm at 875°C.

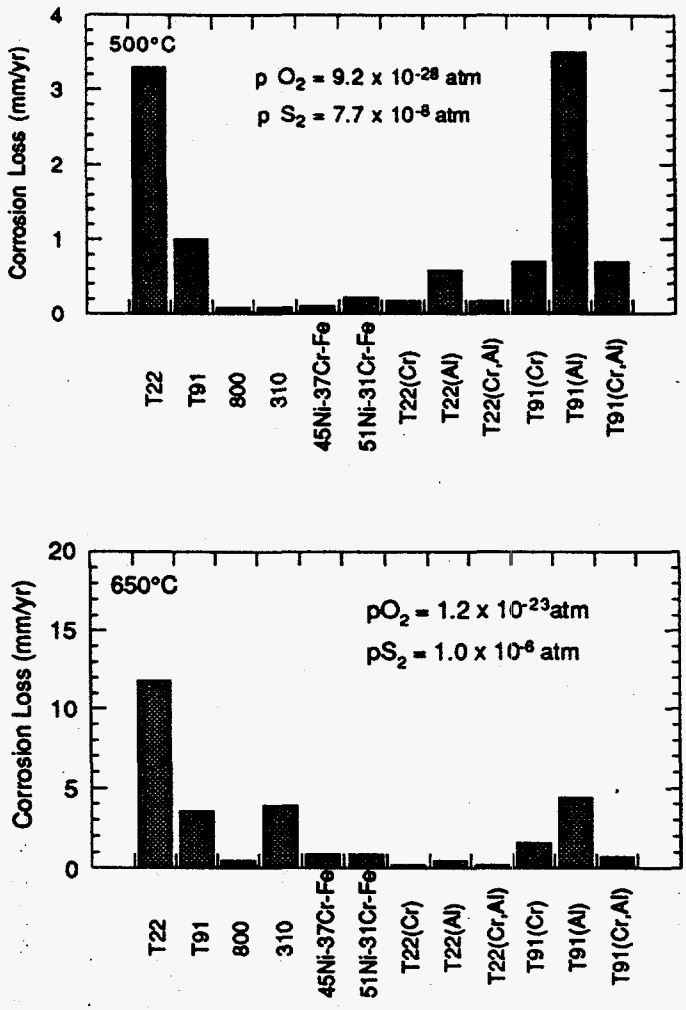

Figure 10. Corrosion loss data for several pack-processed coatings tested in oxygen/sulfur mixed-gas atmospheres at 500°C (top) and 650°C (bottom).

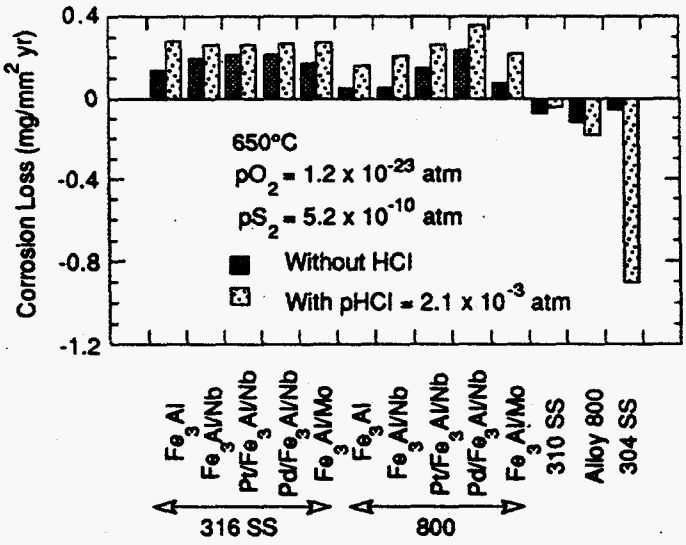

Figure 11. Corrosion loss data for several iron aluminide coatings and uncoated austenitic alloys after exposure in gas mixtures containing H_2S with and without HCl.

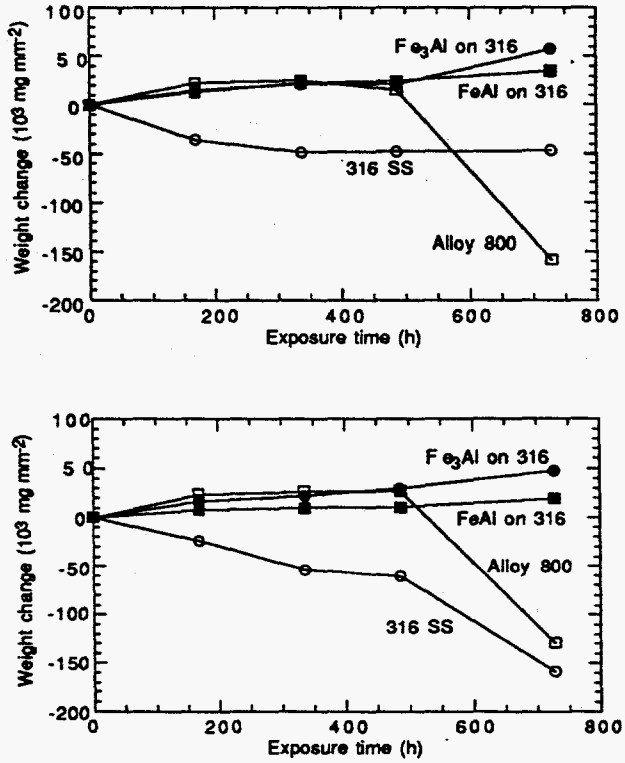

Figure 12. Weight change data for Type 316 stainless steel, Alloy 800, and Fe3Al- and FeAl-coated Type 316 stainless steel after exposure in O/S mixed gas of composition pO_2 = 1.2 x 10^{-23} and pS_2 = 5.2 x 10^{-10} atm at 650°C (top) without HCl and (bottom) with pHCl = 2.1 x 10^{-3} atm.

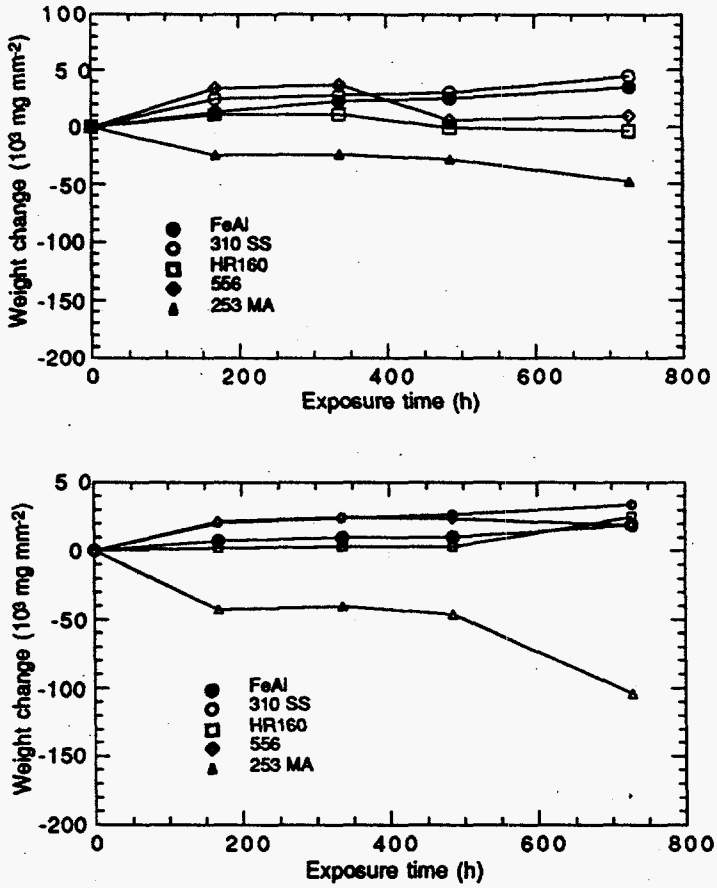

Figure 13. Weight change data for several commercial alloys and FeAl-coated Type 316 stainless steel after exposure in O/S mixed gas of composition $pO_2 = 1.2 \times 10^{-23}$ and $pS_2 = 5.2 \times 10^{-10}$ atm at 650°C (top) without HCl and (bottom) with $pHCl = 2.1 \times 10^{-3}$ atm.

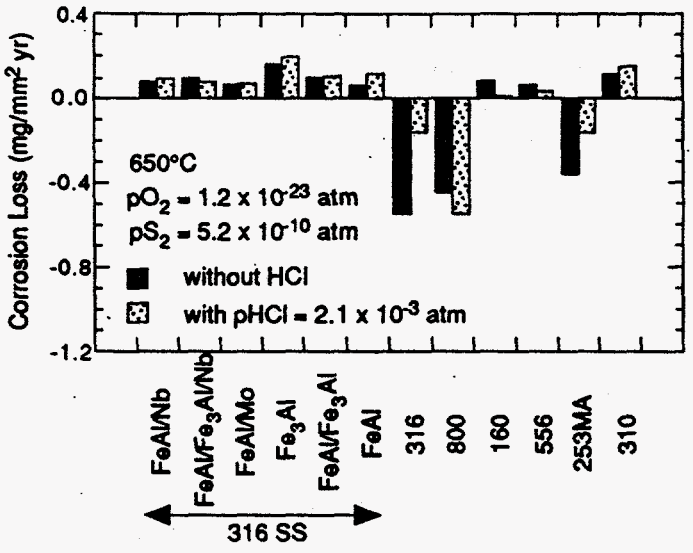

Figure 14. Corrosion loss data for iron aluminide coatings on Type 316 stainless steel and several uncoated high-Cr alloys after exposure in gas mixtures containing H_2S with and without HCl.

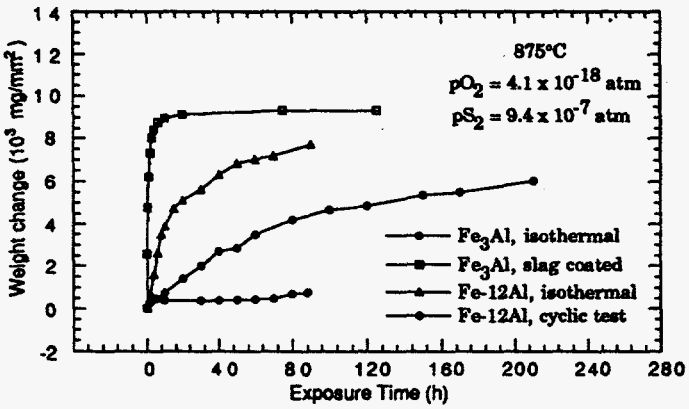

Figure 15. Weight-change data for Fe-12Al binary alloy and Fe_3Al specimens tested in oxygen/sulfur mixed gas at 875°C under thermal cycling conditions and/or in presence of gasifier slag.